Structural modification of twin boundaries in $YBa_2Cu_3O_{6+\eta}$ oxides: Effects of oxygen concentration and temperature

Qingping Meng[1,2] and Yimei Zhu[1,*]
[1]*Department of Condensed Matter Physics and Materials Science, Brookhaven National Laboratory, Upton, New York 11973, USA*
[2]*School of Materials Science and Engineering, Shanghai Jiao Tong University, Shanghai 200030, China*
(Received 27 November 2006; published 2 May 2007)

The modification of the twin boundaries in $YBa_2Cu_3O_{6+\eta}$ due to the oxygen ordering below the temperature of the tetragonal-orthorhombic phase transformation has been studied using mean field theory and spatial gradient terms for the oxygen concentration variation. The distribution of the oxygen atoms across the twin boundaries was calculated at various temperatures and oxygen concentration. Based on these calculations, we deduced the interfacial energy, the equilibrium thickness, and the associated oxygen ordering of the twin boundaries. Their effects on twinning and tweed morphology are also discussed.

DOI: 10.1103/PhysRevB.75.174501 PACS number(s): 74.72.−h, 61.72.Mm

I. INTRODUCTION

Twinning occurs in a broad class of materials, especially perovskite oxides that include ferroelectric, ferroelastic, and superconducting crystals. The existence of the twin domains and twin boundaries (TBs) often affects the physical properties of the materials.[1,2] Twinning frequently is associated with a structural phase transformation. For example, strontium titanate[3,4] ($SrTiO_3$) and fluoroperovskites[5,6] undergo a ferroelastic phase transition from a high-temperature cubic structure to a low-temperature tetragonal structure. Several low-temperature crystallographic variants of equivalent energy are associated with each phase transition. Adjacent variants oriented in different crystallographic directions may be separated from each other by TBs. The most widely used theoretical approach to understanding such transformations is the Devonshire-Ginzburg-Landau (DGL) phenomenological model and its various adaptations.[7–12] In these models, free energy is expressed as a polynomial function of the crystalline strain, the order parameters, and their gradients. Usually, the phase transformations of ferroelectric or ferroelastic crystals are diffusionless; therefore, these order parameters are used to describe spontaneous strain, spontaneous polarization, and displacements of special atomic species.[7,8,10–12] However, other typical phase transformations, whose underlying structural transformations originate from atomic order-disorder transition, are diffusion controlled. These include the cubic to tetragonal phase transformations reflecting the rearrangement of Fe, Pt and Fe, Pd ordering in FePt and FePd alloys;[13] also, oxygen ordering in $YBa_2Cu_3O_{6+\eta}$ superconducting materials causes a tetragonal to orthorhombic structure transformation[2,14,15] (Fig. 1). The structure modification of TBs in $YBa_2Cu_3O_{6+\eta}$ was experimentally observed as a function of oxygen content and dopant concentration.[2,16–20] To understand the change of twin boundaries in this transformation, the process of atomic ordering must be considered. Zhu and Welch[21] studied the TB structure using a Landau expansion including up to fourth-order terms in the oxygen-order parameter; however, their model was too simple to describe the effect of the material composition. Curnoe and Jacobs[22] considered strains as the primary order parameters in their discussion of the evolution of tetragonal-orthorhombic transformation in $YBa_2Cu_3O_{6+\eta}$; apparently, however, using only strains as the order parameters cannot describe the oxygen ordering associated with the transformation. Furthermore, although Semenovskaya and Khachaturyan[23,24] explored the formation of twin domains in this material using mean field theory; the structural variation of TBs was never clarified. In this paper, we focus on our investigations of the structure changes in TBs with composition and temperature. We first discuss our theoretical model, present the free-energy density and the equilibrium conditions in Sec. II and then the solutions for the twin boundaries in Sec. III. Sections IV and V contain, respectively, the numerical calculations, discussions and our conclusions.

II. THEORETICAL MODEL

A. Free energy

Oxygen ordering in $YBa_2Cu_3O_{6+\eta}$ can be described by the redistribution of oxygen atoms over two sublattices of the interstitial site located in the basal Cu-O (001) planes [Fig. 1(a)]. In the disordered tetragonal T phase, oxygen atoms are randomly distributed over α and β sites; therefore, the oxy-

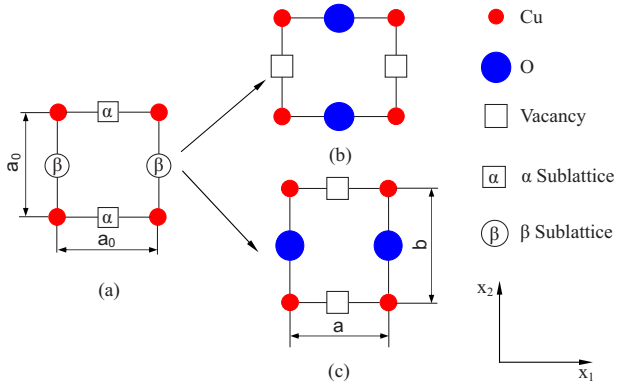

FIG. 1. (Color online) The Cu-O basal plane in $YBa_2Cu_3O_{6+\eta}$. (a) The basal plane of the tetragonal structure, (b) and (c) the orthorhombic structure when oxygen atoms occupy α sites and β sites, respectively.

gen concentrations in these sites are $n_1(\mathbf{r})=n_2(\mathbf{r})=n=\eta/2$. Oxygen ordering entails changes in the oxygen concentration at the α and β sites. Oxygen atoms prefer to occupy one of the sites, and, as they do so, the structure transformation from the tetragonal to the orthorhombic phase occurs concurrently. In the completely ordered state, one of the sites is fully occupied by oxygen atoms while the other is fully vacant, as shown in Figs. 1(b) and 1(c). Here, we consider a two-dimension system with A and B atoms occupying, respectively, the α and β sites [A represents oxygen atoms and B represents vacancies in the basal Cu-O (001) planes of $YBa_2Cu_3O_{6+\eta}$]. n_1 and n_2 are, respectively, the concentration of A atoms in α and β sites. Since the α and β sites are equivalent, Figs. 1(b) and 1(c) are two energetically equivalent variants with different directional orientations. For this system, we write the free-energy density as

$$f = f_1 + f_g = f_c + f_e + f_g. \tag{1}$$

Here $f_1=f_c+f_e$. f_c is the configurational free energy density from A and B atomic distributions with $f_c=E-ST$, where E is the interaction energy of the atoms; S the configurational entropy; and, T is the absolute temperature. If the interactions beyond the third nearest neighbors are ignored, using the mean-field approximation f_c can be written as (see Appendix for details)

$$\begin{aligned} f_c = {} & 2[E_{BB} + (n_1+n_2)(E_{AB}-E_{BB}) + n_1 n_2 v_1] \\ & + \left[E'_{BB} + (n_1+n_2)(E'_{AB}-E'_{BB}) + \tfrac{1}{2}(n_1^2+n_2^2)v_2\right] \\ & + \tfrac{1}{2}k_B T[n_1 \ln n_1 + (1-n_1)\ln(1-n_1) + n_2 \ln n_2 \\ & + (1-n_2)\ln(1-n_2)], \end{aligned} \tag{2}$$

where $v_1=E_{AA}+E_{BB}-2E_{AB}$; $v_2=E'_{AA}+E'_{BB}-2E'_{AB}$; E_{AA}, E_{BB}, and E_{AB} are the pair interaction energy of the nearest-neighbor atoms A-A, B-B, and A-B; and, E'_{AA}, E'_{BB}, and E'_{AB} are those of the second nearest-neighbor atoms. k_B is the Boltzmann constant and f_e is the elastic-energy density. Considering the symmetry of square-rectangular two-dimension transformation, we can write f_e as

$$f_e = \tfrac{1}{2}c_{11}(\varepsilon_{11}^2+\varepsilon_{22}^2) + c_{12}\varepsilon_{11}\varepsilon_{22} + \tfrac{1}{2}c_{44}\varepsilon_{12}^2, \tag{3}$$

where c_{11}, c_{12}, and c_{44} are the elastic constants, and ε_{11}, ε_{22}, and ε_{12} are the strains that are a function of the concentration of A and B atoms in the α and β sites. A simplified approximation is

$$\begin{aligned} \varepsilon_{11} &= \varepsilon_0(n_1-n), \\ \varepsilon_{22} &= \varepsilon_0(n_2-n), \end{aligned} \tag{4}$$

where $\varepsilon_0=\frac{b-a}{b+a}$ $(b>a)$ is a strain constant when the oxygen concentration is known; and n is the averaged concentration of A atoms in α and β sites. In our case, $\varepsilon_{12}=0$. The gradient energy, f_g, for the composition of spatially inhomogeneous configurations is

$$f_g = \tfrac{1}{2}D_{11}(n_{1,1}^2+n_{2,2}^2) + D_{12}n_{1,1}n_{2,2} + \tfrac{1}{2}D_{44}(n_{1,2}+n_{2,1})^2, \tag{5}$$

where D_{11}, D_{12}, and D_{44} are constants; and $n_{i,j}=\frac{\partial n_i}{\partial x_j}$ $(i,j=1,2)$.

B. Equilibrium equations

The total free energy of the system can be expressed as follows:

$$\begin{aligned} F &= \int\int f(n_i,n_{i,j})dx_1dx_2 \\ &= \int\int [f_1(n_i)+f_g(n_{i,j})]dx_1dx_2 \quad (i,j=1,2). \end{aligned} \tag{6}$$

The increase of the free energy arising from a composition fluctuation in an alloy with average concentration n_{i0}, is then given by[25,26]

$$\begin{aligned} \Delta F &= \int\int \Delta f(n_i,n_{i,j})dx_1dx_2 \\ &= \int\int [\Delta f_1(n_i)+f_g(n_{i,j})]dx_1dx_2, \end{aligned} \tag{7}$$

where

$$\Delta f_1 = f_1(n_i) - f_1(n_{i0}) - \sum_i \left[(n_i-n)\left(\frac{\partial f_1}{\partial n_i}\right)_{n_i=n_{i0}}\right]. \tag{8}$$

For our case, the average concentration of n_1 and n_2 is $n_{10}=n_{20}=n$. From the variational derivative of the total free energy, we obtain two static equilibrium differential equations,

$$\frac{\partial}{\partial x_j}\left(\frac{\partial \Delta f}{\partial n_{i,j}}\right) - \frac{\partial \Delta f}{\partial n_i} = 0 \quad (i,j=1,2). \tag{9}$$

The two coupled partial differential equations plus boundary conditions determine the concentration variables n_1 and n_2. Next, we offer special solutions that can used to describe TBs in $YBa_2Cu_3O_{6+\eta}$.

III. TWIN BOUNDARIES

The two-dimensional (2D) TBs we describe here undergo the square-rectangle transformation that consists of {11} planes[27] separating two variants between A atoms preferentially occupying α sites [Fig. 1(b)] and β sites [Fig. 1(c)]. Considering a $(1\bar{1})$ TB, it is convenient to introduce the coordinate system

$$\begin{pmatrix} r \\ s \end{pmatrix} = U\begin{pmatrix} x_1 \\ x_2 \end{pmatrix}, \tag{10}$$

$$U = \begin{pmatrix} \frac{1}{\sqrt{2}} & \frac{1}{\sqrt{2}} \\ -\frac{1}{\sqrt{2}} & \frac{1}{\sqrt{2}} \end{pmatrix}, \tag{11}$$

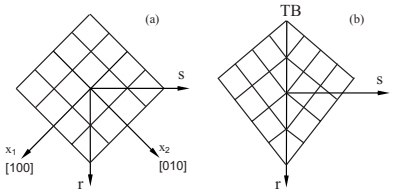

FIG. 2. (a) Two coordinate systems in square parent phase. (b) $(1\bar{1})$ twin boundary at $s=0$ separate two variants of rectangle phase which transform from a square parent phase.

where U represents a rotation of 45° around the axis perpendicular to the x_1x_2 plane, s lies in the direction of the twin boundary normal, and r is the direction parallel to the twin boundary (Fig. 2). In the new coordinate system, we have

$$n_r = \frac{\sqrt{2}}{2}(n_1 + n_2),$$

$$n_s = \frac{\sqrt{2}}{2}(-n_1 + n_2). \tag{12}$$

Based on the symmetry of the twin boundary, for simplicity, we assume that concentration varies only along the s direction. In this circumstance, the problem can be treated as being one dimensional. Thus, from Eq. (9), we obtain

$$\begin{aligned} D_{rs}n_{r,ss} = {} & [2v_1 + v_2 + (c_{11} + c_{12})\varepsilon_0^2](n_r - \sqrt{2}n) \\ & + \frac{\sqrt{2}k_BT}{4}\ln\left(\frac{(n_r - n_s)(n_r + n_s)}{(\sqrt{2}n - n_s)(\sqrt{2}n + n_s)}\right. \\ & \left.\times\frac{(\sqrt{2} - \sqrt{2}n + n_s)(\sqrt{2} - \sqrt{2}n - n_s)}{(\sqrt{2} - n_r + n_s)(\sqrt{2} - n_r - n_s)}\right), \end{aligned} \tag{13}$$

$$\begin{aligned} D_{ss}n_{s,ss} = {} & [-2v_1 + v_2 + (c_{11} - c_{12})\varepsilon_0^2]n_s \\ & + \frac{\sqrt{2}k_BT}{4}\ln\left(\frac{n_r + n_s}{n_r - n_s}\cdot\frac{\sqrt{2} - (n_r - n_s)}{\sqrt{2} - (n_r + n_s)}\right) \\ & - \frac{\sqrt{2}k_BT}{4}(n_r - \sqrt{2}n)\left(\frac{1}{\sqrt{2}n + n_s} - \frac{1}{\sqrt{2}n - n_s}\right. \\ & \left. + \frac{1}{\sqrt{2} - (\sqrt{2}n + n_s)} - \frac{1}{\sqrt{2} - (\sqrt{2}n - n_s)}\right), \end{aligned} \tag{14}$$

where $D_{rs} = \frac{1}{2}(D_{11} - D_{12})$ and $D_{ss} = \frac{1}{2}(D_{11} + D_{12} + 2D_{44})$. For the twin structure, the composition is uniform at far from twin boundaries, i.e., $n_r = \frac{\sqrt{2}}{2}(n_1 + n_2) = \sqrt{2}n$ at $s \to \pm\infty$. Therefore, Eq. (13) only has a trivial solution of $n_r = \sqrt{2}n$. Then Eq. (14) becomes

$$\begin{aligned} D_{ss}n_{s,ss} = {} & [-2v_1 + v_2 + (c_{11} - c_{12})\varepsilon_0^2]n_s \\ & + \frac{\sqrt{2}k_BT}{4}\ln\left(\frac{\sqrt{2}n + n_s}{\sqrt{2}n - n_s}\cdot\frac{\sqrt{2}(1-n) + n_s}{\sqrt{2}(1-n) - n_s}\right). \end{aligned} \tag{15}$$

Although simplifications have been made in Eq. (15), it does not have an analytic solution. We give approximate solutions as follows.

A. The solution near T_c^-

At a temperature slightly lower than the critical temperature of order-disorder transition, T_c^-, the concentrations of A atoms in the α and β sites deviate only marginally from the average value, i.e., n_s is a small quantity compared with n. Taylor expansion, including up to fifth-order terms, was applied to the second item of the right-hand side of Eq. (15). Then, Eq. (15) can be rewritten as

$$D_{ss}n_{s,ss} = An_s + Bn_s^3 + Cn_s^5, \tag{16}$$

where

$$A = -2v_1 + v_2 + (c_{11} - c_{12})\varepsilon_0^2 + \frac{1}{2}\frac{k_BT}{n(1-n)}, \tag{17a}$$

$$B = \frac{k_BT}{12}\left(\frac{1}{n^3} + \frac{1}{(1-n)^3}\right), \tag{17b}$$

$$C = \frac{k_BT}{40}\left(\frac{1}{n^5} + \frac{1}{(1-n)^5}\right). \tag{17c}$$

Several authors[12,28–30] employed Eq. (16) to study diffusionless transformations, such as martensitic,[29,30] ferroelastic,[12] and ferroelectric transformation.[28] Usually, they assumed that the coefficient A is a linear function of temperature, and that B and C are constants. For $YBa_2Cu_3O_{6+\eta}$, they represent functions of oxygen concentration and of temperature, as shown in Eqs. (17). From Eq. (17b), we know that $B>0$. Therefore, Eq. (16) describes a second-order square-rectangular transition.[30] The square state ($n_s=0$) is stable when $A>0$; the rectangular state $n_s=\pm n_{s0}$ is stable when $A<0$, where

$$n_{s0} = \pm\left(\frac{-B + \sqrt{B^2 - 4AC}}{2C}\right)^{1/2}. \tag{18}$$

The critical temperature, T_c, is determined for $A=0$,

$$T_c = -\frac{2n(1-n)[-2v_1 + v_2 + (c_{11} - c_{12})\varepsilon_0^2]}{k_B}. \tag{19}$$

Below the critical temperature, there is a rectangular-rectangular soliton solution of Eq. (16),

$$n_s = \frac{n_{s0}\sinh(\kappa s)}{[\cosh^2(\kappa s) + \lambda]^{1/2}}, \tag{20}$$

where

$$\lambda = \frac{2(A + Bn_{s0}^2)}{4A + Bn_{s0}^2}, \tag{21a}$$

$$\kappa = \left(-\frac{2A + Bn_{s0}^2}{2D_{ss}}\right)^{1/2}. \tag{21b}$$

hence, the values of κ and λ, depending on the concentration, n, and temperature, T, determine the thickness and shape of a twin boundary between two rectangular phases.

B. Solution for an arbitrary temperature below T_c

For a system with uniform composition at an arbitrary temperature below the critical temperature, T_c, we need to solve Eq. (15) to determine the distribution of oxygen concentration. Usually only numerical solutions can be obtained from Eq. (15). First, we determine the boundary condition of Eq. (15) by assuming that the composition of the system is homogeneous in regions far away from the twin boundary. That is

$$\lim_{s\to\pm\infty}\frac{dn_s}{ds}=0. \tag{22}$$

Equation (15) then becomes

$$[-2v_1+v_2+(c_{11}-c_{12})\varepsilon_0^2]n_s + \frac{\sqrt{2}k_BT}{4}\ln\left(\frac{\sqrt{2}n+n_s}{\sqrt{2}n-n_s}\cdot\frac{\sqrt{2}(1-n)+n_s}{\sqrt{2}(1-n)-n_s}\right)=0. \tag{23}$$

This equation is the same as that derived from the mean-field theory. The equilibrium value, n_s, i.e., n_{s0}, can be calculated from Eq. (23) at $s\to\pm\infty$. In this case, solving Eq. (15) becomes a two-point boundary value problem in ordinary differential equations. However, unlike the initial value problem of an ordinary differential equation, a two-point boundary value problem may not have a solution, or may have a finite number, or even an infinite number of solutions. To derive reasonable solutions from Eq. (15), a trial resolution for the solution desired should be provided. Equation (20) is used for the trial solution, after substituting the n_{s0} in Eq. (20) by the result calculated from Eq. (23).

IV. CALCULATED RESULTS AND DISCUSSION

Using the elastic constants of $YBa_2Cu_3O_7$ (Ref. 31) $c_{11}=3.9\times10^{12}$ dyn/cm^2; $c_{22}=1.36\times10^{12}$ dyn/cm^2, strain $\varepsilon_0=0.009$, unit-cell volume $V=173$ Å^3, and the oxygen interaction data given by Semenovskaya and Khachaturyan's [23,24], we obtain $v_1=1758k_B$ K, and $v_2=1668k_B$ K. The critical temperature T_c can be determined from Eq. (19) with $T_c=794$ K for $n=0.5$ ($YBa_2Cu_3O_7$), and $T_c=323$ K for $n=0.115$ ($YBa_2Cu_3O_{6.23}$). The gradient coefficient D_{ss} is considered as a constant; its value is estimated by the thickness of the TB.[32] Previous reports suggest that the TB's thickness[33–35] in $YBa_2Cu_3O_{6+\eta}$ and its alloys, $YBa_2(Cu_{0.98}M_{0.02})O_{6+\eta}$, is about 0.7–2.6 nm at room temperature. Consistent with the Zhu *et al.* experimental results,[33,34] we assume $D_{ss}=100k_B$ (K nm^2) in our calculations, a value that will give rise to a reasonably thick twin boundary. From Eq. (12), we know that $\sqrt{2}n_s=n_2-n_1$, which represents the order degree of the system. For example, with $\sqrt{2}n_s=1$ for $n=0.5$, then, it means that $n_2=1$, i.e., all oxygen atoms occupy the β sites shown in Fig. 1(c), and vice versa at $\sqrt{2}n_s=-1$, $n_1=1$, that is, all oxygen atoms occupy the α sites shown in Fig. 1(b). Figure 3 depicts the distribution of oxygen concentration across the TB with various average oxygen concentrations and temperatures. From Eqs. (4), (10), and (11), we obtain the normal strain

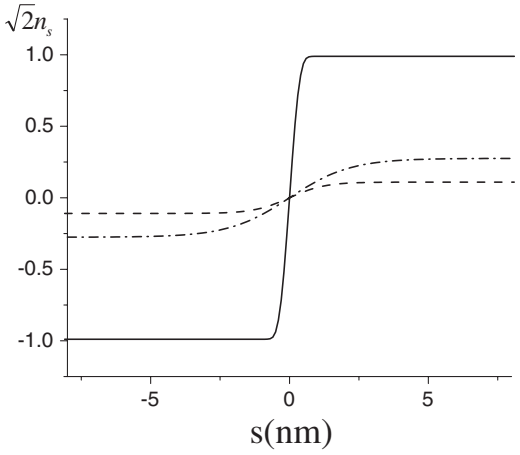

FIG. 3. The distribution of oxygen concentration across TB. Solid line is for $n=0.5$, $T=300$ K; dashed—dotted line is for $n=0.5$, $T=774$ K; and dashed line is for $n=0.115$, $T=300$ K.

$$\varepsilon_{ss}=\varepsilon_{rr}=\tfrac{1}{2}(\varepsilon_{11}+\varepsilon_{22})=0, \tag{24}$$

and the shear strain

$$\varepsilon_{sr}=\frac{1}{2}(-\varepsilon_{11}+\varepsilon_{22})=\frac{1}{2}\varepsilon_0(-n_1+n_2)=\frac{\sqrt{2}}{2}\varepsilon_0 n_s, \tag{25}$$

i.e., the shear strain ε_{sr} has a linear relationship with n_s.

Using Cahn and Hilliard's method,[25] the thickness of the TB can be calculated by

$$d=\frac{2n_{s0}}{\left(\frac{dn_s}{ds}\right)_{x=0}}. \tag{26}$$

The TB's energy density also can be calculated by

$$\sigma=2\int_{-\infty}^{\infty}D_{ss}\left(\frac{dn_s}{ds}\right)^2 ds. \tag{27}$$

Figure 4 shows the calculated results for $n=0.5$. Other concentrations give similar results. Figure 3 and Fig. 4 clearly demonstrate that the thickness of TBs under a constant oxygen concentration will rapidly decrease, i.e., they will become sharper and sharper with a decrease in temperature, but their energy will correspondingly increase.

An associated microstructure, the so-called tweed structure, which often is related to structural disorder and transition, has been observed in a wide variety of materials.[16–20,35–40] Usually, it is argued that the tweed pattern is a precursor phenomenon to a structural transformation, and arises in direct response to statistically significant compositional fluctuations.[41,42] In $YBa_2Cu_3O_{6+\eta}$, tweed is often considered as microtwins. In oxygen deficient $YBa_2Cu_3O_{6.23}$ (Ref. 16) and alloyed $YBa_2Cu_3O_{6+\eta}$ (Refs. 16–20, 35, and 40) (substituting Cu with transition-metal elements, such as Fe and Co), the tweed structures appear at room temperature. The structure of tweed also involves a small shear strain in the $\{1\ 1\ 0\}$ plane along the $\langle\bar{1}10\rangle$ direction, that is strain ε_{sr}; the interfacial width between two domains of a tweedy structure is large. From electron micros-

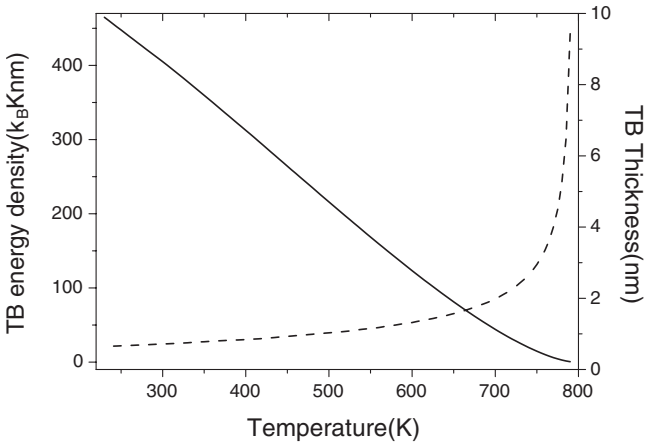

FIG. 4. TB energy density (solid line) and thickness (dashed line) vs temperature for $n=0.5$.

copy contrast analysis, it was suggested[20] that the strain from one domain to another across a TB is large and abrupt, but that across the tweed is small and gradual, i.e., a TB across two twin variants in $YBa_2Cu_3O_{6+\eta}$ is sharper and narrower than the tweed boundary across two tweed variants. Figure 5 is a schematic drawing of twin and tweed structures. Our theoretical calculations in Fig. 3 indicate that the TB structure gently changes from one side to the other side when the temperature is slightly below T_c, such as depicted by the dashed-dotted line shown at 774 K in $n=0.5$ ($YBa_2Cu_3O_7$) with $T_c=794$ K, and the dashed line at 300 K for $n=0.115$ ($YBa_2Cu_3O_{6.23}$) with $T_c=323$ K; in contrast, the solid line representing the TB at 300 K for $n=0.5$, is much sharper when the temperature is significantly below T_c. The TB structures depicted by the dashed-dotted and dashed lines in Fig. 3 match the experimental observations for the tweed structure. Therefore, we conclude that tweed structure can form at temperatures slightly below T_c, and that twins form at significantly below T_c.

Semenovskaya *et al.*[23,24,43] and Parlinski *et al.*[44,45] considered that the tweed structure is not an equilibrium phase but rather a nonequilibrium or metastable configuration. Computer simulations by Semenovskaya *et al.* showed that the tweed structure is an intermediate one as the distribution of oxygen gradually evolves through an ordering process. Parlinski *et al.* reported that the recognizable embryos of the tweed structure result from thermal fluctuations above the transition temperature. They thought that the reason for the appearance of a metastable tweed pattern at room temperature is that the dopant atoms prevent coarsening of order domain and the ability of oxygen to diffuse is low at room temperature. Our theoretical analysis indicates that the tweed structure may be a stable configuration in $YBa_2Cu_3O_{6+\eta}$. Several experiments[16–20,46–50] support our conclusion; Poberaj *et al.*[46] and Veal *et al.*[47–49] measured observable oxygen diffusion in $YBa_2Cu_3O_{6+\eta}$ at room temperature and the tweed structure observed by Zhu *et al.*[16] in $YBa_2Cu_3O_{6.23}$ at room temperature and by Schwarz *et al.*[50] in $YBa_2Cu_3O_{6.68}$ at 723 K. Both the tweed structure may be equilibrium and stable.

The equilibrium TB spacing can be estimated by [51,52]

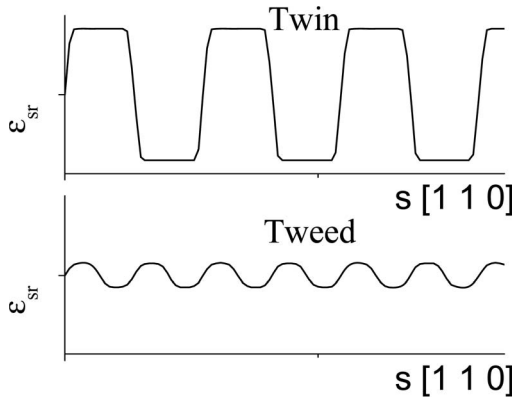

FIG. 5. Schematics of tweed and twin structure.

$$D \sim \left(\frac{g\gamma}{M\phi^2}\right)^{1/2}, \tag{28}$$

where M is the elastic modulus, g is the length of the crystal grain along the twin boundary, γ is the boundary energy, and ϕ is the transformation strain,[52] i.e.,

$$\phi = \varepsilon_{22} - \varepsilon_{11} = \sqrt{2}\varepsilon_0 n_{s0}. \tag{29}$$

Equation (25) is used to deduce Eq. (29). Some authors[21,53,54] considered that ϕ is a constant. However, in our analysis, ϕ exhibits similar changes as n_{s0} with oxygen concentration and temperature. Using Eqs. (28) and (29), we can estimate the ratios of TB spacing between $YBa_2Cu_3O_7$ and $YBa_2Cu_3O_{6.23}$ at 300 K (ignoring changes in M and g with oxygen composition). γ is $405k_B$ (K·nm) in $YBa_2Cu_3O_7$ and $1.26k_B$(K·nm) in $YBa_2Cu_3O_{6.23}$; n_{s0} is 0.6997 in $YBa_2Cu_3O_7$ and 0.0775 in $YBa_2Cu_3O_{6.23}$ at 300 K. We obtain $D_1/D_2 \approx 2$. D_1 is the TB spacing in $YBa_2Cu_3O_7$; and D_2 is that in $YBa_2Cu_3O_{6.23}$. Based on experimental observations,[2] the TB spacing is about 80–260 nm in $YBa_2Cu_3O_7$ ($n=0.5$) at room temperature. Therefore, we estimated "TB" (tweed) spacing in $YBa_2Cu_3O_{6.23}$ at 300 K is about 40–130 nm. The tweed spacing from experimental observation[2,16] in $YBa_2Cu_3O_{6.23}$ at 300 K is about 25 nm, which is in agreement with our theoretical estimation.

The present work was aimed at elucidating the twin boundary structure in the high-temperature superconductor $YBa_2Cu_3O_{6+\eta}$. The relationship between twin boundaries and superconducting critical temperature is not well understood. Fang *et al.*[55] discussed the possibility that the twin boundary region is an area of higher superconducting critical temperature than the matrix, while Deutscher and Müller[56] proposed that the twin boundary layer is weakly superconducting. Based on our results, $|n_s|$ in a twin boundary is less than its value far from a twin boundary, i.e., the degree of oxygen order in twin boundaries is lower than that in a crystal matrix. The superconductivity of $YBa_2Cu_3O_{6+\eta}$ depends on the degree of oxygen order, and the material can change from a superconductor to an insulator with the reduction of the order. The reduction of the degree of order of oxygen atoms at TBs results in a reduction of the oxygen-hole concentration,[21] thus resulting in the reduction of local superconductivity in comparison to the matrix. Hence, we ex-

pect that, depending on the degree of disorder at TBs (or the sharpness of the TB), in $YBa_2Cu_3O_{6+\eta}$, especially in fully oxidized samples, TBs can play a significant role in determining local superconductivity. For instance, they can act as either a pinning center, or a channel for superconducting vortices, depending on whether the vortices move perpendicular, or parallel, to the TBs. Several experiments[57–59] are consistent with our results.

V. CONCLUSIONS

We have presented a theoretical model for the twin boundary (TB) structural modification during square-rectangular structural transformations arising from oxygen ordering in $YBa_2Cu_3O_{6+\eta}$. The changes of TB structures associated with oxygen concentration and temperature were studied. At temperatures slightly below the phase transition T_c, we found a solitary wave solution to describe the structural evolution of TB. For an arbitrary temperature below the oxygen-ordering temperature, we used the solitary wave solution as a trial solution to calculate numerically the TB structure, including its thickness and energy. Our findings indicate that the thickness of the TB decrease rapidly, while their energy increases with a decrease of temperature when the oxygen concentration remains constant. We also found that the degree of oxygen ordering at TB is lower than that in the crystal matrix. Based on our analysis, the TB related tweed structure may be explained as being a thermodynamically stable structure in pure and doped $YBa_2Cu_3O_{6+\eta}$ systems.

ACKNOWLEDGMENTS

This work was performed under the auspices of the Division of Materials Science, Office of Basic Energy Sciences, US Department of Energy under Contract No. DE-AC02-98CH10886. Valuable discussions with D. O. Welch are also acknowledged.

APPENDIX: THE CONFIGURATIONAL FREE ENERGY DENSITY

The nearest-neighbor interactions are those of an atomic pair on α-β sites. From Fig. 1, the A-A, B-B, and A-B atomic pair numbers of the nearest neighborhood are, respectively,

$$N_{AA} = \tfrac{1}{2}n_1 N_\alpha \cdot 4n_2 + \tfrac{1}{2}n_2 N_\beta \cdot 4n_1 = 4n_1 n_2 N, \tag{A1}$$

$$N_{BB} = 4(1-n_1)(1-n_2)N, \tag{A2}$$

$$N_{AB} = 4(n_1 + n_2 - 2n_1 n_2)N, \tag{A3}$$

where N_α and N_β correspond to the number of α and β lattice sites. In the case of Fig. 1, $N_\alpha = N_\beta = N$. The nearest-neighbor interaction energy is

$$E_1 = 4N[E_{BB} + (n_1 + n_2)(E_{AB} - E_{BB}) + n_1 n_2 v_1]. \tag{A4}$$

The second nearest-neighbor interactions are those of the four atomic pairs of α-α sites (Fig. 1). There are two pairs across a middle atom and two without a middle atom. The A-A, B-B, and A-B atomic-pairs' interaction energy of the nearest neighborhood are, respectively,

$$V'_{AA} = (n_1^2 + n_2^2)N(v_{AA}^1 + v_{AA}^2) = (n_1^2 + n_2^2)NE'_{AA}, \tag{A5}$$

$$V'_{BB} = [2 + 2(n_1 + n_2) + n_1^2 + n_2^2]NE'_{BB}, \tag{A6}$$

$$V'_{AB} = 2(n_1 + n_2 - n_1^2 - n_2^2)NE'_{AB}, \tag{A7}$$

where $E'_{AA} = v_{AA}^1 + v_{AA}^2$ and v_{AA}^1 is the interaction energy of the A-A atomic pair across a middle atom; v_{AA}^2 is that without a middle atom. E'_{BB} and E'_{AB} are similar. The second nearest-neighbor interaction energy is

$$E_2 = 2N\left[E'_{BB} + (n_1 + n_2)(E'_{AB} - E'_{BB}) + \tfrac{1}{2}(n_1^2 + n_2^2)v_2\right]. \tag{A8}$$

The configurational entropy is

$$S = k_B \ln\left(\frac{N!}{(n_1 N)![(1-n_1)N]!} \cdot \frac{N!}{(n_2 N)![(1-n_2)N]!}\right). \tag{A9}$$

Using Stirling's approximation, the configurational entropy is rewritten

$$S = -k_B N[n_1 \ln n_1 + (1-n_1)\ln(1-n_1) + n_2 \ln n_2 + (1-n_2)\ln(1-n_2)]. \tag{A10}$$

Combined with (A4), (A8), and (A10), we obtain

$$f_c = \frac{F_c}{2N} = 2[E_{BB} + (n_1 + n_2)(E_{AB} - E_{BB}) + n_1 n_2 v_1] + \left(E'_{BB} + (n_1 + n_2)(E'_{AB} - E'_{BB}) + \frac{1}{2}(n_1^2 + n_2^2)v_2\right) + \frac{1}{2}k_B T[n_1 \ln n_1 + (1-n_1)\ln(1-n_1) + n_2 \ln n_2 + (1-n_2)\ln(1-n_2)]. \tag{A11}$$

*Corresponding author; Electronic address: zhu@bnl.gov

[1] F. Jona and G. Shirane, *Ferroelectric Crystals* (Dover, New York, 1993).

[2] Z. Cai and Y. Zhu, *Microstructures and Structural Defects in High-Temperature Superconductors* (World Scientific, River Edge, NJ, 1998).

[3] H. Unoki and T. Sakudo, J. Phys. Soc. Jpn. **23**, 546 (1967).

[4] P. A. Fleury, J. F. Scott, and J. M. Worlock, Phys. Rev. Lett. **21**, 16 (1968).

[5] A. Okazaki and Y. Suemune, J. Phys. Soc. Jpn. **16**, 671 (1961).

[6] M. Rousseau, J. Y. Gesland, J. Julliard, and J. Nouet, Phys. Rev. B **12**, 1579 (1975).

[7] A. F. Devonshire, Philos. Mag. **40**, 1040 (1949).
[8] A. F. Devonshire, Philos. Mag. **42**, 1065 (1951).
[9] L. D. Landau and E. M. Lifshitz, *Statistical Physics* (Butterworth-Heineman, Oxford, 1980), Vol. 1.
[10] E. K. H. Salje, *Phase Transition in Ferroelastic and Co-Elastic Crystals* (Cambridge University Press, Cambridge, 1990).
[11] J. C. Tolédano and P. Tolédano, Phys. Rev. B **21**, 1139 (1980).
[12] W. Cao and G. R. Barsch, Phys. Rev. B **41**, 4334 (1990).
[13] B. Zhang, M. Lelovic, and W. A. Soffa, Scr. Metall. Mater. **25**, 1577 (1991).
[14] D. de Fontaine, L. T. Wille, and S. C. Moss, Phys. Rev. B **36**, 5709 (1987).
[15] A. G. Khachaturyan, S. V. Semenovskaya, and J. W. Morris, Jr., Phys. Rev. B **37**, 2243 (1988).
[16] Y. Zhu, M. Suenaga, and A. R. Moodenraugh, Philos. Mag. Lett. **62**, 51 (1990).
[17] Y. Zhu, M. Suenaga, and J. Tafto, Philos. Mag. Lett. **64**, 29 (1991).
[18] Y. Zhu, M. Suenaga, and J. Tafto, Philos. Mag. A **67**, 573 (1993).
[19] Y. Zhu and J. M. Cowley, Philos. Mag. A **69**, 397 (1994).
[20] Y. Zhu, M. Suenaga, and A. R. Moodenbaugh, Ultramicroscopy **37**, 341 (1991).
[21] Y. Zhu and D. O. Welch, "The nature of twin boundaries in the high-temperature superconductor $YBa_2Cu_3O_{7-\delta}$," in *Advances in Twinning*, edited by S. Ankem and C. S. Pande (A Publication of TMS, 1999).
[22] S. H. Curnoe and A. E. Jacobs, Phys. Rev. B **64**, 064101 (2001).
[23] S. Semenovskaya and A. G. Khachaturyan, Phys. Rev. Lett. **67**, 2223 (1991).
[24] S. Semenovskaya and A. G. Khachaturyan, Phys. Rev. B **46**, 6511 (1992).
[25] J. W. Cahn and J. E. Hilliard, J. Chem. Phys. **28**, 258 (1958).
[26] R. Poduri and L.-Q. Chen, Acta Mater. **44**, 4253 (1996).
[27] J. Sapriel, Phys. Rev. B **12**, 5128 (1975).
[28] J. Lajzerowicz, Ferroelectrics **35**, 219 (1981).
[29] F. Falk, Z. Phys. B: Condens. Matter **51**, 177 (1983); **54**, 159 (1984).
[30] A. E. Jacobs, Phys. Rev. B **31**, 5984 (1985).
[31] R. C. Baetzold, Phys. Rev. B **38**, 11304 (1988).
[32] D. Shilo, G. Ravichandran, and K. Bhattacharya, Nat. Mater. **3**, 453 (2004).
[33] Y. Zhu, M. Suenaga, J. Tafto, and D. O. Welch, Phys. Rev. B **44**, 2871 (1991).
[34] Y. Zhu, M. Suenaga, Y. Xu, R. L. Sabatini, and A. R. Moodenbaugh, Appl. Phys. Lett. **54**, 374 (1989).
[35] Y. Xu, M. Suenaga, J. Tafto, R. L. Sabatini, A. R. Moodenbaugh, and P. Zolliker, Phys. Rev. B **39**, 6667 (1989).
[36] L. E. Tanner, Philos. Mag. **14**, 111 (1966).
[37] I. M. Robertson and C. M. Wayman, Philos. Mag. A **48**, 421 (1983); **48**, 443 (1983); **48**, 629 (1983).
[38] D. H. Jack, Acta Matell. **24**, 137 (1976).
[39] S. Muto, S. Takeda, R. Oshima, and F. E. Fujita, J. Phys.: Condens. Matter **1**, 9971 (1989).
[40] W. W. Schmahi, A. Putnis, E. Salje, P. Freeman, A. Graemebarber, R. Jones, K. K. Singh, J. Blunt, P. P. Edwards, J. Loram, and K. Mirza, Philos. Mag. Lett. **60**, 241 (1989).
[41] S. Kartha, T. Castán, J. A. Krumhansl, and J. P. Sethna, Phys. Rev. Lett. **67**, 3630 (1991).
[42] S. Kartha, J. A. Krumhansl, J. P. Sethna, and L. K. Wickham, Phys. Rev. B **52**, 803 (1995).
[43] S. Semenovskaya, Y. Zhu, M. Suenaga, and A. G. Khachaturyan, Phys. Rev. B **47**, 12182 (1993).
[44] K. Parlinski, V. Heine, and E. K. H. Salje, J. Phys.: Condens. Matter **5**, 497 (1993).
[45] K. Parlinski, E. K. H. Salje, and V. Heine, Acta Metall. Mater. **41**, 839 (1993).
[46] I. Poberaj, D. Mihailović, and S. Bernik, Phys. Rev. B **42**, 393 (1990).
[47] B. W. Veal, H. You, A. P. Paulikas, H. Shi, Y. Fang, and J. W. Downey, Phys. Rev. B **42**, 4770 (1990).
[48] J. D. Jorgensen, S. Pei, P. Lightfoot, H. Shi, A. P. Paulikas, and B. W. Veal, Physica C **167**, 571 (1990).
[49] R. Mogilevsky, R. Levi-Setti, B. Pashmakov, L. Liu, K. Zhang, H. M. Jaeger, D. B. Buchholz, R. P. H. Chang, and B. W. Veal, Phys. Rev. B **49**, 6420 (1994).
[50] W. Schwarz, O. Blaschko, G. Collin, and F. Marucco, Phys. Rev. B **48**, 6513 (1993).
[51] A. G. Khachaturyan, *Theory of Structure Transformation in Solids* (Wiley, New York, 1983).
[52] A. L. Roitburd, Sov. Phys. Solid State **10**, 2870 (1969).
[53] S. K. Streiffer, E. M. Zielinski, B. M. Lairson, and J. C. Bravman, Appl. Phys. Lett. **58**, 2171 (1991).
[54] L. S. Chumbley, J. D. Verhoeven, M. R. Kim, A. L. Cornelius, and M. J. Kramer, IEEE Trans. Magn. **25**, 2337 (1989).
[55] M. M. Fang, V. G. Kogan, D. K. Finnemore, J. R. Clem, L. S. Chumbley, and D. E. Farrell, Phys. Rev. B **37**, 2334 (1988).
[56] G. Deutscher and K. A. Müller, Phys. Rev. Lett. **59**, 1745 (1987).
[57] G. P. E. M. van Bakel, P. A. Hof, J. P. M. van Engelen, P. M. Bronsveld, and J. Th. M. De Hosson, Phys. Rev. B **41**, 9502 (1990).
[58] Y. Yan, W. Y. Liang, T. Walther, and W. M. Stobbs, Phys. Rev. B **54**, 16234 (1996).
[59] L. Wu, S. V. Solovyov, H. J. Wiesmann, D. O. Welch, and M. Suenaga, Supercond. Sci. Technol. **16**, 1127 (2003).